Invariant Natural Killer T cell dynamics in HIV-associated tuberculosis

Naomi F. Walker[1,2,3,4] PhD, Charles Opondo PhD[5], Graeme Meintjes[1,3] PhD, Nishta Jhilmeet[1] PhD, Jon S Friedland[6] FMedSci, Paul T Elkington[2,7] FRCP, Robert J Wilkinson[1,3,8,9] F Med Sci, Katalin A Wilkinson[1,3,8] PhD.

[1]Wellcome Centre for Infectious Diseases Research in Africa, Institute of Infectious Disease and Molecular Medicine, University of Cape Town, Observatory 7925, Republic of South Africa

[2]Infectious Diseases and Immunity, and Imperial College Wellcome Trust Centre for Global Health, Imperial College London, W12 0NN, United Kingdom

[3]Department of Medicine, University of Cape Town, Observatory 7925, Republic of South Africa

[4]TB Centre and Department of Clinical Research, London School of Hygiene and Tropical Medicine, Keppel St, London, WC1E 7HT, United Kingdom

[5]Department of Medical Statistics, London School of Hygiene and Tropical Medicine, Keppel St, London, WC1E 7HT, United Kingdom

[6]Institute of Infection & Immunity, St. George's, University of London, London, SW17 0RE, United Kingdom

[7]NIHR Biomedical Research Centre, School of Clinical and Experimental Sciences, Faculty of Medicine, University of Southampton, Southampton, SO16 6YD, United Kingdom

[8]The Francis Crick Institute, London, NW1 1AT, United Kingdom

[9]Department of Medicine, Imperial College London, W2 1PG, United Kingdom

Running title: *Invariant Natural Killer T cells in TB-IRIS*

Address for correspondence:
Dr Katalin Wilkinson
The Francis Crick Institute
1 Midland Road, London NW1 1AT
Email: katalin.wilkinson@crick.ac.uk

Alternative corresponding author:
Dr Naomi F. Walker
London School of Hygiene and Tropical Medicine
Keppel Street, London, WC1E 7HT
Email: naomi.walker@lshtm.ac.uk

Word Count: 2988
Abstract word count: 231
Key words: invariant Natural Killer T cell; HIV; tuberculosis; paradoxical immune reconstitution inflammatory syndrome (IRIS); innate.

Key points

iNKT cells were depleted in patients with advanced HIV infection, most significantly immunoregulatory CD4+ subsets.

In patients with HIV-associated TB who developed TB-IRIS, iNKT cells were elevated with increased degranulation compared to non-IRIS patients, implicating iNKT cells in TB-IRIS immunopathology.

Abstract

Rationale: Tuberculosis (TB) is the leading cause of mortality and morbidity in people living with HIV infection. HIV-infected patients with TB disease are at risk of the paradoxical TB-associated immune reconstitution inflammatory syndrome (TB-IRIS) when they commence anti-retroviral therapy. However, the pathophysiology is incompletely understood and specific therapy is lacking.

Objectives: We investigated the hypothesis that invariant Natural Killer T (iNKT) cells contribute to innate immune dysfunction associated with TB-IRIS.

Methods: In a cross-sectional study of 101 HIV-infected and -uninfected South African patients with active TB and controls, iNKT cells were enumerated using α-galactosylceramide-loaded CD1d tetramers and subsequently functionally characterised by flow cytometry. In a second study of 49 HIV-1-infected TB patients commencing anti-retroviral therapy, iNKT cells in TB-IRIS patients with non-IRIS controls were compared longitudinally.

Measurements and main results: Circulating iNKT cells were reduced in HIV-1 infection, most significantly the CD4+ subset, which was inversely associated with HIV-1 viral load. iNKT cells in HIV-associated TB had increased surface CD107a expression, indicating cytotoxic degranulation. Relatively increased iNKT cell frequency in HIV-infected patients with active TB was associated with development of TB-IRIS following anti-retroviral therapy initiation. iNKT cells in TB-IRIS were CD4+CD8- subset deplete and degranulated around the time of TB-IRIS onset.

Conclusions: Reduced iNKT cell CD4+ subsets as a result of HIV-1 infection may skew iNKT cell functionality towards cytotoxicity. Increased CD4- cytotoxic iNKT cells may contribute to immunopathology in TB-IRIS.

Introduction

Tuberculosis (TB) causes 1.6 million deaths annually and is the leading cause of death in HIV-1 infected people (1). Anti-retroviral therapy (ART) naive HIV-1-infected patients with TB are at risk of the paradoxical TB immune reconstitution inflammatory syndrome (TB-IRIS) after commencing ART (2). Paradoxical TB-IRIS is characterised by an acute inflammatory response to *Mycobacterium tuberculosis* (Mtb) presenting as a clinical deterioration in a patient already receiving TB treatment, typically around two weeks post ART initiation (3). Paradoxical TB-IRIS is difficult to manage, frequently requiring non-specific immunosuppression with corticosteroids. Risk factors include disseminated TB and low CD4 T cell count at ART initiation, but the pathophysiology is incompletely defined (4). Recent studies have identified potential contributory innate immune mechanisms, including neutrophil recruitment, inflammasome activation and proinflammatory cytokine excess (5-10). These potential mechanisms have been recently reviewed (2)

Invariant natural killer T (iNKT) cells are a T cell subset that bridge innate and adaptive immunity, therefore are of interest in TB-IRIS pathogenesis (11). Distinct from NK cells and conventional T cells, iNKT cells express an invariant T cell receptor comprised of Vα24 and Vβ11 in humans, and specifically recognise CD1d-presented lipid antigens, responding on activation with rapid cytokine production. Additionally, iNKT cells recognise and are potently activated by the marine sponge glycolipid α-galactosylceramide (α-galcer), bound to CD1d (12, 13).

Mtb cell wall is lipid-rich and therefore CD1d-presented molecules that activate iNKT cells may have a role in host immunity to Mtb (14, 15). *In vitro*, iNKT cells directly restricted Mtb growth and were bactericidal (16). In mice, augmenting iNKT cell responses with α-galcer

97 improved BCG vaccine efficacy and anti-tuberculosis treatment responses (17, 18). In non-
98 human primates, increased iNKT cell frequency was associated with TB resistance (19). In
99 humans, a limited number of studies have demonstrated numerical and functional defects of
100 iNKT cells in active TB (20-23).
101
102 We previously reported elevated expression of cytotoxic mediators, perforin and granzyme B,
103 in peripheral blood mononuclear cells (PBMC) in response to Mtb antigen stimulation and
104 elevated frequencies of cytotoxic cells expressing CD3 and Vα24 T cell receptor in TB-IRIS
105 patients compared to non-IRIS controls, suggesting that iNKT cells may play a role in TB-IRIS
106 (24). Here, we systematically investigated iNKT cells in cross-sectional and longitudinal
107 studies addressing the hypothesis that iNKT cell dysfunction contributes to TB-IRIS
108 immunopathology. We describe for the first time iNKT cell aberration in HIV-associated TB
109 disease and increased cytotoxic iNKT cells in TB-IRIS patients.
110
111 **Methods**
112 Full methods are provided in the online supplement.
113 *Study Participants*
114 The study was approved by the University of Cape Town Human Research Ethics Committee
115 (REF 516/2011). All participants provided written informed consent. Cross-sectional study
116 participants were retrospectively designated into four categories:
117 1) HIV-uninfected patients without active TB (HIV-TB-)
118 2) HIV-uninfected patients with a new diagnosis of active TB (HIV-TB+)
119 3) ART naïve, HIV-infected patients without active TB (HIV+TB-)
120 4) ART naïve, HIV-infected patients with a new diagnosis of active TB (HIV+TB+).
121 Longitudinal study participants were ART naïve HIV-1-infected patients with a CD4 count

<200 cells/μL and recently diagnosed TB. Longitudinal study visits occurred at TB diagnosis (TB0), ART initiation (ARV0), two (ARV2) and four (ARV4) weeks of ART and if new symptoms suggesting TB-IRIS occurred. TB-IRIS diagnosis was assigned retrospectively on expert case review, using consensus criteria (3).

iNKT cell enumeration and characterisation

PBMC were isolated over Ficoll and cryopreserved. Cells were rapidly thawed in warmed RPMI/10% FCS, before viability staining with Violet LIVE/DEAD© Fixable stain kit (VIVID, Invitrogen, Paisley, UK), then washed and re-suspended for incubation with either α-galcer-loaded CD1d tetramer or control CD1d tetramer (Proimmune, Oxford, UK) for 30 minutes on ice, protected from light. Subsequently, cells were washed, stained with antibody mastermix 1 (Supplementary Table S1) for 30 minutes at 4^{o}C, washed and re-suspended in PBS, 1% Hi-FCS and 2% paraformaldehyde, then incubated for 1 hour, washed and resuspended for acquisition.

Data acquisition and analysis

Data were acquired on an LSRFortessa^{TM} (BD Biosciences, USA) and analysed using Flowjo software (Tree Star, Ashland, OR). iNKT cells were defined as CD3+ CD19- CD1d α-galcer tet+ Vβ11+ T cells. The gating strategy is shown in Figure 1A. iNKT cell frequency was calculated as a percentage of CD3+ CD19- live lymphocytes, with subtraction of the equivalent tetramer negative control proportion, and reported per million CD3+CD19- live lymphocytes. iNKT cell numbers were calculated by multiplying the iNKT cell frequency as a percentage of live lymphocytes with the total lymphocyte count per millilitre of peripheral blood (22).

Statistical analysis was performed using Prism 6 (GraphPad, UK) and STATA 14. Unadjusted non-parametric analyses were by two-tailed Fisher's Exact or Mann–Whitney U, or for comparisons of more than two groups, by Kruskal-Wallis with Dunn's multiple comparisons test. In the cross-sectional study, we used a multivariable linear regression model to investigate differences in iNKT cell frequency and in percentage iNKT cell CD4/CD8 expression by disease category. In the longitudinal study, a multivariable negative binomial model was fitted to examine associations of iNKT cell frequency and number with TB-IRIS status, and a multivariate linear regression model to estimate difference in CD4/CD8 cell subset percentages between TB IRIS and non-IRIS patients.

Results

PBMC samples were available from 101 patients (see Table 1). HIV+TB+ patients compared to HIV+TB- patients had lower total CD4 counts but similar CD4 percentages, and higher HIV-1 viral loads. In HIV+TB+ compared to HIV-TB+, there were trends towards reduced cavitary (p=0.067), but increased miliary (p=0.051) and extra-pulmonary (p=0.054) TB presentation, indicating reduced destructive pulmonary pathology but more widely disseminated TB disease in HIV-infected patients (25).

Circulating iNKT cells are depleted in HIV-1 infection and active TB

In an unadjusted analysis, comparing iNKT cell frequency in HIV-1-infected and -uninfected patients, with and without active TB, we found that iNKT cell frequency was reduced in HIV+TB+ (p=0.001) and HIV+TB- (p=0.005) compared to HIV-TB- patients (Figure 1B and Table 2). Example plots are shown in Supplementary Figure S1. A similar pattern was observed in comparison of iNKT cell numbers (iNKT cells per ml, Figure 1C) and reduction in iNKT cells numbers was found in HIV-TB+ compared to HIV-TB- patients (p=0.044). Linear

regression comparing HIV-TB+, HIV+TB- and HIV+TB+ to HIV-TB- provided further evidence of association between reduced iNKT cell frequency in HIV+TB- (p=0.023) and HIV+TB+ (p=0.024) after adjustment for age and sex, but there was no evidence of a reduction in iNKT cell frequency in HIV-TB+ compared to HIV-TB- (p=0.301).

CD4+ iNKT cell subsets are depleted in HIV-1 infection

iNKT cells may exist as CD4+CD8-, CD4-CD8+, CD8+CD4+, or double negative (DN) subsets. CD4+ iNKT cells secrete both Th1 and Th2 cytokines and may be immunoregulatory, whilst CD8+ iNKT cells and DN iNKT cell subsets predominantly secrete Th1 cytokines and have increased cytotoxic functionality (26, 27). Unadjusted analyses showed that HIV-1 infection was associated with lower CD4+ iNKT cell percentages (Figure 2A) and frequency (CD4+ iNKT cells per million CD3+ CD19- live lymphocytes, Figure 2B) in patients with (p=0.007) and without (p=0.005) active TB. Active TB did not clearly reduce CD4+ iNKT cell percentage, but was associated with reduced CD4+ iNKT cell frequency in HIV-uninfected patients (Figure 2B, p=0.016). In HIV-infected patients, total iNKT cell frequency did not correlate with peripheral blood CD4 T cell count, peripheral blood CD4 T cell percentage or HIV-1 viral load. However, CD4+ iNKT cell percentage was correlated with total peripheral blood CD4 T cell count (Figure 2C, r=0.456, p=0.001) and there was an inverse correlation with HIV-1 viral load (Figure 2D, r=-0.571, p<0.001), indicating most severe depletion of CD4+ iNKT cells occurred in advanced HIV infection.

Next, we examined CD4 and CD8 co-expression on iNKT cells. In HIV-TB-, we found CD4+CD8- (Figure 2E) and DN iNKT cells (Figure 2F) to be the predominant iNKT cell subsets constituting a median of 42.1% and 43.7% of the iNKT cell population respectively. However, compared to HIV-TB- patients, HIV-infected patients had reduced percentages of

CD4+CD8- iNKT cells, constituting a median of only 1.55% iNKT cells in HIV+TB+ ($p<0.001$). In HIV-infected patients, there was a trend towards an increased percentage of CD4-CD8- iNKT cells (Figure 2F) and CD4-CD8+ iNKT cells (not shown), compared to HIV uninfected patients. To explore this further, we performed regression analysis comparing CD4/CD8 iNKT cell percentages in each group to HIV-TB-, adjusting for age and sex (Supplementary Table S2). This analysis showed evidence of reduced CD4+CD8- iNKT cells in HIV+TB- and HIV+TB+ compared to HIV-TB- ($p<0.001$ for both) and increased CD4-CD8- percentage in HIV+TB- ($p=0.010$). CD4-CD8+ cells were increased in HIV+TB- ($p=0.037$) and HIV+TB+ ($p=0.016$) compared to HIV-TB-. For CD4/CD8 subset iNKT cell frequencies, see Supplementary Figure S2.

iNKT cells in HIV-associated TB are pro-inflammatory with a cytotoxic phenotype

There was high iNKT cell surface expression of the maturation marker, CD161, CD95 and PD1 in HIV+TB+, but not more than in the control groups (data not shown). We investigated iNKT cell degranulation by measuring CD107a surface expression (28). CD107a+ iNKT cells were increased in HIV+TB+ patients, compared to HIV+TB- patients, suggesting increased cytotoxic degranulation (Figure 3A), but this phenotype was not observed in all HIV+TB+ patients. To explore this further, we investigated association between CD107a+ iNKT cell positivity and TB disease phenotype in HIV+TB+. We found significantly increased CD107a+ iNKT cell percentage in HIV+TB+ patients with clinical features of extrapulmonary TB compared to those without, consistent with the hypothesis that disseminated Mtb might lead to peripheral blood iNKT cell degranulation (Figure 3B).

In summary, we found that HIV infection was associated with iNKT cell depletion and CD4+ iNKT cell subsets were most significantly depleted in advanced HIV. Active TB was associated with a modest reduction in iNKT cell number in HIV-uninfected patients, but did not clearly reduce iNKT cell frequency. The immunoregulatory CD4+CD8- iNKT cell subset, the predominant subset in the healthy repertoire, was depleted in HIV-infected patients with and without active TB. CD4-CD8+ and DN iNKT cells were the dominant iNKT cell subsets in HIV-infected patients. There were increased CD107a+ iNKT cell percentages in HIV-infected patients with active TB, indicating a cytotoxic phenotype, which was associated with extra-pulmonary TB.

iNKT cell frequency is increased in TB-IRIS patients

Next, in a longitudinal study, we evaluated iNKT cells in patients with advanced HIV and recently diagnosed TB, who commenced TB treatment and then ART, and were at risk of paradoxical TB-IRIS. Fifty-seven participants were enrolled. Clinical features of this cohort have previously been reported (25). Paradoxical TB-IRIS was diagnosed in 29 (59.2%) patients. Participants were included if PBMC were available at least one study timepoint (TB0, ARV0, ARV2 and ARV4) and there was follow up to ARV12. One participant was excluded as no PBMC samples were available, another as they were an elite controller and therefore likely to be immunologically distinct, and a third due to hepatotoxicity on TB treatment resulting in a significant delay to ART initiation. The subsequent analysis reports findings from 29 TB-IRIS patients and 17 non-IRIS controls. Patient demographics and TB diagnosis are provided in Table 3 and were not significantly different comparing TB-IRIS with non-IRIS patients. Between ARV0 and ARV4, peripheral blood CD4 T cell counts increased ($p<0.001$) from median 101 cells/μl to 206 cells/μl in TB-IRIS patients and from 99 cells/μl to 175 cells/μl in non-IRIS patients.

First, we enumerated iNKT cells. We found an elevated iNKT cell frequency in TB-IRIS compared to non-IRIS patients (Figure 4A). At ARV2, the most frequent time of TB-IRIS presentation, the median iNKT cell frequency per million CD3+CD19- live lymphocytes in TB-IRIS was 992 (IQR, 166-5682) compared to 100 (IQR 24.5-440) in non-IRIS patients (p=0.025 in unadjusted analysis). Multivariable modelling including data from timepoints ARV0, ARV2 and ARV4 demonstrated a significant association between TB-IRIS and increased iNKT cell frequency, adjusted for age and sex (p=0.022, Supplementary Table S3), but no increase in iNKT cell frequency over time and the association did not differ with total peripheral blood CD4 T cell count, nor HIV viral load. A similar trend was found for iNKT cell numbers in the adjusted logistic regression analysis (p=0.062, Supplementary Figure S3).

iNKT cell function and phenotype in TB-IRIS

Next, we examined CD4/CD8 iNKT cell subsets in the longitudinal study. CD4+ iNKT cell percentage and frequency were low, both in TB-IRIS and non-IRIS patients and did not increase in the first four weeks of ART, despite an increased peripheral blood CD4 T cell count. CD4+CD8- iNKT cell percentage was significantly lower in TB-IRIS patients than non-IRIS patients, (p=0.015 by multivariate linear regression modelling, Figure 4B). Supplementary Figure S4 shows CD4/CD8 subset frequency demonstrating a predominance of DN and CD4-CD8+ iNKT cells in TB-IRIS compared to non-IRIS patients, at ARV2 (p=0.029 and p=0.036 respectively).

In both TB-IRIS and non-IRIS patients, CD161+ iNKT cell and CD107a+ iNKT cell percentages were dynamic (Supplementary Figure 5 A-B). CD95 cell surface expression, indicative of cytotoxicity, and PD1+ iNKT cell percentages were high both in TB-IRIS and

non-IRIS patients whilst CD40L+ iNKT cell percentages were relatively low, possibly indicating iNKT cell exhaustion (Supplementary Figure S5 C-E) (22, 29). In TB-IRIS, CD161+ iNKT cell percentages decreased between ARV0 and ARV2, suggesting a loss of mature iNKT cells, whereas in non-IRIS patients, iNKT cell CD161 positivity was similar (Figure 5A). In TB-IRIS patients, CD107a+ iNKT cells increased between ARV0 and ARV2 relative to non-IRIS patients, suggesting degranulation occurred at the time of IRIS symptom onset (Figure 5B). CD107a+ iNKT cell frequency was increased in TB-IRIS compared to non-IRIS patients at ARV2 (Figure 5C).

In summary, patients with advanced HIV and active TB had low circulating iNKT cell frequency pre-ART initiation, but iNKT cell populations were skewed towards pro-inflammatory, cytotoxic subsets. Higher iNKT cell frequency was associated with TB-IRIS following ART initiation and iNKT cells in TB-IRIS patients were CD4+CD8- subset deplete, with increased DN and CD4-CD8+ iNKT cell frequency at the time of TB-IRIS onset. Increased CD107a+ iNKT cell subsets in TB-IRIS patients also at ARV2 suggested increased iNKT cell degranulation occurring at the time of TB-IRIS presentation.

Discussion

In this study, we demonstrated low iNKT cell frequency in ART-naïve patients with advanced HIV infection, with a paucity of CD4+ iNKT cells, and relatively increased proportions of CD4-CD8- iNKT cells, representing a shift from CD4+ subsets found in HIV-uninfected patients. Decreased iNKT cell numbers and CD4+ iNKT cell frequency were associated with active TB in patients without HIV infection, but this finding was not consistent in HIV-infected patients. In HIV-infected patients with active TB, increased degranulation of iNKT cells was found. Despite low iNKT cell frequencies in these patients, there were relatively increased

iNKT cells in patients who went on to develop TB-IRIS compared to those who did not and these were predominantly DN or CD4-CD8+ iNKT cells. There was no significant recovery in peripheral blood CD4+ iNKT cells in the first four weeks of ART, despite increased peripheral blood CD4 count (25).

Our findings are consistent with prior human studies measuring iNKT cells in HIV infection, which report reduced iNKT cell frequency in HIV-infected patients (23, 30, 31). A previous study demonstrated that *in vitro* HIV-1 infection directly infects and selectively depletes CD4+ iNKT cells. Activated iNKT cells were more susceptible to HIV-1 infection than conventional CD4 T cells. (32). In HIV-leprosy co-infection, iNKT cell populations were found to be reduced more profoundly than in leprosy or HIV infection alone (33). iNKT cell activation due to mycobacterial infection might exacerbate iNKT cell depletion in HIV-1 infected patients. Although we found the lowest iNKT cell frequency and numbers in patients with HIV-1 infection and active TB, active TB did not clearly have an additive effect of iNKT cell depletion in HIV-infected patients.

There are a number of potential mechanisms by which iNKT cells may contribute to immunopathology in TB-IRIS. They may directly recognise foreign or self lipid antigens presented via CD1d, or become activated by local cytokine networks (26). Once activated iNKT cells may rapidly secrete proinflammatory cytokines and chemokines promoting CD4 T cell expansion, activation and neutrophil infiltration, features of TB-IRIS we have previously shown, in addition to causing cell death (5, 6, 9, 10, 26, 34). Ultimately, this cascade may lead to MMP activation and tissue destruction, in turn propagating proinflammatory cytokine secretion in the vicious cycle of hyperinflammation that is the hallmark of TB-IRIS (7, 25).

iNKT cell quantification using α-galcer-loaded CD1d-loaded tetramers, is recognised as a stringent method of iNKT cell quantification (35, 36). However, we cannot extrapolate our findings beyond the limitations of this methodology, which may be affected by TCR downregulation on activation, nor beyond peripheral blood into tissue compartments (35). It is possible that increased circulating iNKT cells in TB-IRIS patients represents failure of migration to tissues. We found evidence of increased iNKT cell degranulation in extra-pulmonary TB, compared to pulmonary TB, raising the possibility that more abundant, disseminated Mtb antigen may drive iNKT cell degranulation in HIV-associated TB and increased iNKT cell cytotoxicity in TB-IRIS patients (24).

As a rare T cell subset, iNKT cells have formerly been difficult to study and iNKT cell function in infection is a relatively understudied area. However, in the field of oncology, adjuvants to boost iNKT cell cytotoxicity have been the focus of translational research and have entered early phase clinical trials (37, 38). Our study suggests that boosting iNKT cell cytotoxicity would not be an appropriate strategy in HIV-associated TB. However, an improved understanding of the role of iNKT cells in TB immunopathology could identify novel therapeutic targets. As human and mouse iNKT cell physiology differ, further human clinical and cellular studies are required, including study of iNKT cells in tissue compartments.

Conclusion

This study supports a role for iNKT cells in innate immune dysfunction in paradoxical TB-IRIS. We have shown profound CD4+ iNKT cell subset depletion in advanced HIV-1 infection and a lesser effect of active TB in HIV-uninfected patients. In patients with advanced HIV and a new diagnosis of active TB, iNKT cell populations were skewed towards a proinflammatory, cytotoxic phenotype. Patients who developed TB-IRIS had increased iNKT cells compared to

non-IRIS patients and iNKT cell degranulation occurred at the time of IRIS, potentially contributing to immunopathology.

Author Contributions

N.F.W., G.M., R.J.W., J.S.F., P.T.E. and K.A.W. conceived and designed the clinical study. N.F.W., G.M., and R.J.W. recruited the clinical cohort. N.F.W. N.J. R.J.W. and K.A.W. conceived and designed the cellular studies. N.F.W. and K.A.W. conducted the cellular studies. N.F.W and C.O. performed data analysis. N.F.W and K.A.W. hold all primary data and are responsible for the integrity of the data. All authors contributed to the writing of the manuscript and approved the final submitted version.

Funding

NFW received funding from Wellcome (094000) and The British Federation of Women Graduates (Elizabeth Bowden scholarship), and is currently supported by a National Institute for Health Research Academic Clinical Lecturership, the British Infection Association (Research Project Grant), and a Starter Grant for Clinical Lecturers (The Academy of Medical Sciences UK, Wellcome, Medical Research Council UK, British Heart Foundation, Arthritis Research UK, Royal College of Physicians and Diabetes UK); GM was supported by Wellcome (098316 and 203135/Z/16/Z), the South African Research Chairs Initiative of the Department of Science and Technology and National Research Foundation (NRF) of South Africa (Grant No 64787), NRF incentive funding (UID: 85858) and the South African Medical Research Council through its TB and HIV Collaborating Centres Programme with funds received from the National Department of Health (RFA# SAMRC-RFA-CC: TB/HIV/AIDS-01-2014); RJW and KAW receive support from the Francis Crick Institute which is supported by Wellcome (FC001218), Medical Research Council (FC001218) and CRUK (FC001218), and the European Union Horizon 2020 research and innovation programme under grant agreement no. 643381; RJW receives additional support from Wellcome (104803, 203135) and the National Institutes of Health (U01AI115940); NJ was supported by Wellcome (088316) and The South African National Research Foundation (443386).

Acknowledgements

We thank S. Mansour for review of the draft manuscript.

References

1. WHO. Global tuberculosis report 2018. World Health Organisation, Geneva, Switzerland, 2018.

2. Walker NF, Stek C, Wasserman S, Wilkinson RJ, Meintjes G. The tuberculosis-associated immune reconstitution inflammatory syndrome: recent advances in clinical and pathogenesis research. Curr Opin HIV AIDS. 2018;13(6):512-21.

3. Meintjes G, Lawn SD, Scano F, Maartens G, French MA, Worodria W, et al. Tuberculosis-associated immune reconstitution inflammatory syndrome: case definitions for use in resource-limited settings. Lancet Infect Dis. 2008;8(8):516-23.

4. Namale PE, Abdullahi LH, Fine S, Kamkuemah M, Wilkinson RJ, Meintjes G. Paradoxical TB-IRIS in HIV-infected adults: a systematic review and meta-analysis. Future Microbiol. 2015;10(6):1077-99.

5. Lai RP, Meintjes G, Wilkinson KA, Graham CM, Marais S, Van der Plas H, et al. HIV-tuberculosis-associated immune reconstitution inflammatory syndrome is characterized by Toll-like receptor and inflammasome signalling. Nature Commun. 2015;6:8451.

6. Tadokera R, Meintjes G, Skolimowska KH, Wilkinson KA, Matthews K, Seldon R, et al. Hypercytokinaemia accompanies HIV-tuberculosis immune reconstitution inflammatory syndrome. Eur Respir J. 2011;37(5):1248-59.

7. Tadokera R, Meintjes GA, Wilkinson KA, Skolimowska KH, Walker N, Friedland JS, et al. Matrix metalloproteinases and tissue damage in HIV-tuberculosis immune reconstitution inflammatory syndrome. Eur J Immunol. 2014;44(1):127-36.

8. Andrade BB, Singh A, Narendran G, Schechter ME, Nayak K, Subramanian S, et al. Mycobacterial antigen driven activation of CD14++CD16- monocytes is a predictor of tuberculosis-associated immune reconstitution inflammatory syndrome. PLoS Pathog. 2014;10(10):e1004433.

9. Marais S, Wilkinson KA, Lesosky M, Coussens AK, Deffur A, Pepper DJ, et al. Neutrophil-Associated Central Nervous System Inflammation in Tuberculous Meningitis Immune Reconstitution Inflammatory Syndrome. Clin Infect Dis. 2014;59(11):1638-47.

10. Nakiwala JK, Walker NF, Diedrich CR, Worodria W, Meintjes G, Wilkinson RJ, et al. Neutrophil Activation and Enhanced Release of Granule Products in HIV-TB Immune Reconstitution Inflammatory Syndrome. J Acquir Immune Defic Syndr. 2018;77(2):221-9.

11. Taniguchi M, Seino K, Nakayama T. The NKT cell system: bridging innate and acquired immunity. Nat Immunol. 2003;4(12):1164-5.

12. Kim CH, Johnston B, Butcher EC. Trafficking machinery of NKT cells: shared and differential chemokine receptor expression among Valpha 24(+)Vbeta 11(+) NKT cell subsets with distinct cytokine-producing capacity. Blood. 2002;100(1):11-6.

13. Godfrey DI, Stankovic S, Baxter AG. Raising the NKT cell family. Nat Immunol. 2010;11(3):197-206.

14. De Libero G, Mori L. The T-Cell Response to Lipid Antigens of Mycobacterium tuberculosis. Front Immunol. 2014;5:219.

15. Fischer K, Scotet E, Niemeyer M, Koebernick H, Zerrahn J, Maillet S, et al. Mycobacterial phosphatidylinositol mannoside is a natural antigen for CD1d-restricted T cells. Proc Natl Acad Sci U S A. 2004;101(29):10685-90.

16. Sada-Ovalle I, Chiba A, Gonzales A, Brenner MB, Behar SM. Innate invariant NKT cells recognize *Mycobacterium tuberculosis*-infected macrophages, produce interferon-gamma, and kill intracellular bacteria. PLoS Pathog. 2008;4(12):e1000239.

17. Venkataswamy MM, Baena A, Goldberg MF, Bricard G, Im JS, Chan J, et al. Incorporation of NKT cell-activating glycolipids enhances immunogenicity and vaccine efficacy of *Mycobacterium bovis* bacillus Calmette-Guerin. J Immunol. 2009;183(3):1644-56.

18. Sada-Ovalle I, Skold M, Tian T, Besra GS, Behar SM. Alpha-galactosylceramide as a therapeutic agent for pulmonary *Mycobacterium tuberculosis* infection. Am J Respir Crit Care Med. 2010;182(6):841-7.

19. Chancellor A, White A, Tocheva AS, Fenn JR, Dennis M, Tezera L, et al. Quantitative and qualitative iNKT repertoire associations with disease susceptibility and outcome in macaque tuberculosis infection. Tuberculosis (Edinb). 2017;105:86-95.

20. Montoya CJ, Catano JC, Ramirez Z, Rugeles MT, Wilson SB, Landay AL. Invariant NKT cells from HIV-1 or *Mycobacterium tuberculosis*-infected patients express an activated phenotype. Clin Immunol. 2008;127(1):1-6.

21. Sutherland JS, Jeffries DJ, Donkor S, Walther B, Hill PC, Adetifa IMO, et al. High granulocyte/lymphocyte ratio and paucity of NKT cells defines TB disease in a TB-endemic setting. Tuberculosis. 2009;89(6):398-404.

22. Kee SJ, Kwon YS, Park YW, Cho YN, Lee SJ, Kim TJ, et al. Dysfunction of Natural Killer T Cells in Patients with Active Mycobacterium tuberculosis Infection. Infect Immun. 2012;80(6):2100-8.

23. Paquin-Proulx D, Costa PR, Terrassani Silveira CG, Marmorato MP, Cerqueira NB, Sutton MS, et al. Latent Mycobacterium tuberculosis Infection Is Associated With a Higher Frequency of Mucosal-Associated Invariant T and Invariant Natural Killer T Cells. Front Immunol. 2018;9:1394.

24. Wilkinson KA, Walker NF, Meintjes G, Deffur A, Nicol MP, Skolimowska KH, et al. Cytotoxic mediators in paradoxical HIV-tuberculosis immune reconstitution inflammatory syndrome. J Immunol. 2015;194(4):1748-54.

25. Walker NF, Wilkinson KA, Meintjes G, Tezera LB, Goliath R, Peyper JM, et al. Matrix Degradation in Human Immunodeficiency Virus Type 1-Associated Tuberculosis and Tuberculosis Immune Reconstitution Inflammatory Syndrome: A Prospective Observational Study. Clin Infect Dis. 2017;65(1):121-32.

26. Brennan PJ, Brigl M, Brenner MB. Invariant natural killer T cells: an innate activation scheme linked to diverse effector functions. Nat Rev Immunol. 2013;13(2):101-17.

27. Chen CY, Huang D, Wang RC, Shen L, Zeng G, Yao S, et al. A critical role for CD8 T cells in a nonhuman primate model of tuberculosis. PLoS Pathog. 2009;5(4):e1000392.

28. Zeng SG, Ghnewa YG, O'Reilly VP, Lyons VG, Atzberger A, Hogan AE, et al. Human invariant NKT cell subsets differentially promote differentiation, antibody production, and T cell stimulation by B cells in vitro. J Immunol. 2013;191(4):1666-76.

29. Liu TY, Uemura Y, Suzuki M, Narita Y, Hirata S, Ohyama H, et al. Distinct subsets of human invariant NKT cells differentially regulate T helper responses via dendritic cells. Eur J Immunol. 2008;38(4):1012-23.

30. van der Vliet HJJ, von Blomberg BME, Hazenberg MD, Nishi N, Otto SA, van Benthem BH, et al. Selective Decrease in Circulating Vα24+Vβ11+ NKT Cells During HIV Type 1 Infection. J Immunol. 2002;168(3):1490-5.

31. van der Vliet HJ, van Vonderen MG, Molling JW, Bontkes HJ, Reijm M, Reiss P, et al. Cutting edge: Rapid recovery of NKT cells upon institution of highly active antiretroviral therapy for HIV-1 infection. J Immunol. 2006;177(9):5775-8.

32. Motsinger A, Haas DW, Stanic AK, Van Kaer L, Joyce S, Unutmaz D. CD1d-restricted human Natural Killer T cells are highly susceptible to human immunodeficiency virus 1 infection. J Exp Med. 2002;195(7):869-79.

33. Carvalho KI, Bruno FR, Snyder-Cappione JE, Maeda SM, Tomimori J, Xavier MB, et al. Lower numbers of Natural Killer T cells in HIV-1 and *Mycobacterium leprae* co-infected patients. Immunology. 2012;136(1):96-102.

34. Marais S, Lai RPJ, Wilkinson KA, Meintjes G, O'Garra A, Wilkinson RJ. Inflammasome Activation Underlying Central Nervous System Deterioration in HIV-Associated Tuberculosis. J Infect Dis. 2017;215(5):677-86.

35. Berzins SP, Smyth MJ, Baxter AG. Presumed guilty: Natural Killer T cell defects and human disease. Nat Rev Immunol. 2011;11(2):131-42.

36. Brossay L, Chioda M, Burdin N, Koezuka Y, Casorati G, Dellabona P, et al. CD1d-mediated recognition of an alpha-galactosylceramide by natural killer T cells is highly conserved through mammalian evolution. J Exp Med. 1998;188(8):1521-8.

480 37. Nair S, Dhodapkar MV. Natural Killer T Cells in Cancer Immunotherapy. Front Immunol.
481 2017;8:1178.
482 38. Shissler SC, Bollino DR, Tiper IV, Bates JP, Derakhshandeh R, Webb TJ. Immunotherapeutic
483 strategies targeting natural killer T cell responses in cancer. Immunogenetics. 2016;68(8):623-38.

484

485

Figure Legends

Figure 1 Reduced iNKT cells in HIV-1 infection and active TB

iNKT cells were enumerated by flow cytometry using α-galcer loaded CD1d tetramers. Each sample was stained in parallel with a control tetramer (without α-galcer) to identify non-specific tetramer binding for subtraction. The gating strategy shown in (A) demonstrates an iNKT cell frequency of 0.77%, with no control tetramer binding, equivalent to 7700 cells per million CD3+CD19- live lymphocytes. Decreased iNKT cell frequency (B) was found in HIV-infected patients with active TB (HIV+TB+) and without active TB (HIV+TB-), compared to HIV-uninfected patients without active TB (HIV-TB-). Similarly, in HIV-infected patients with and without active TB, decreased iNKT cell numbers (cells per millilitre peripheral blood (C)) were found compared to HIV-uninfected patients without active TB. Additionally, in HIV-uninfected patients with active TB (HIV-TB+), iNKT cell numbers were reduced compared to HIV-uninfected patients without TB. Analysis was by Kruskal Wallis with Dunn's multiple comparison's test to calculate adjusted p values: *$p<0.05$; **$p<0.01$; ***$p<0.001$. In (B) and (C), zero values were replaced by one for representation on a log scale.

Figure 2 CD4+ iNKT cell subset depletion in HIV-1-associated TB

HIV-infected patients, most significantly those with active TB, had depleted CD4+ iNKT cells as measured by percentage of total iNKT cell count (A) and frequency per million CD3+ CD19- live lymphocytes (B). In HIV-infected patients, peripheral blood CD4 T cell count positively correlated with CD4+ iNKT cell percentage (C). HIV-1 viral load negatively correlated with CD4+ iNKT cell percentage (D). In HIV-uninfected patients without active TB, iNKT cells were mostly either CD4+ CD8- or double negative (CD4-CD8-), whilst in HIV-infected patients CD4+ CD8- iNKT cells were depleted and double negative iNKT cells were the predominant subset (E, F). Analysis was by Kruskal Wallis with Dunn's multiple comparisons

test to calculate multiplicity-adjusted p values: * $p<0.05$; ** $p<0.01$; *** $p<0.001$ or by Spearman's correlation (C, D).

Figure 3 iNKT cell cytotoxicity in HIV-associated TB

In HIV-associated TB, there were increased percentages of CD107a+ iNKT cells, suggestive of cytotoxic degranulation (A). In HIV-infected patients with clinical features of extra-pulmonary TB (EPTB), there were increased CD107a+ iNKT cell percentages compared to HIV-infected patients with pulmonary TB (B). Analysis was by Kruskal Wallis with Dunn's multiple comparisons test to calculate multiplicity-adjusted p values or by Mann-Whitney U in (D): * $p<0.05$.

Figure 4 iNKT cells are elevated in TB-IRIS patients and are CD4+CD8- subset deplete

iNKT cells were enumerated longitudinally by flow cytometry using α-galcer loaded CD1d tetramers, in a cohort of 46 HIV-1-infected patients with active TB. Samples were collected around the time of TB diagnosis (TB0), at anti-retroviral therapy initiation (ARV0, a median of 17.5 days post TB treatment initiation) and at two weeks (ARV2) and four weeks (ARV4) post-ART initiation although not all patients contributed data to the first timepoint as patients who had taken more than four doses of TB treatment at enrolment contributed data from ARV0, resulting in fewer data points at TB0. TB-IRIS presentation was typically at ARV2. Increased iNKT cell frequency (A) was observed in TB-IRIS patients compared to non-IRIS controls. CD4+CD8- iNKT cell percentages were reduced in TB-IRIS patients (B). Statistical analysis was by multivariable negative binomial modelling to examine associations of iNKT cell frequency and number with TB-IRIS status and by multivariate linear regression modelling to estimate difference in CD4/CD8 cell subset percentages between TB IRIS and non-IRIS

patients, including data from all timepoints to derive p values which are reported on the corresponding figure. In (A), zero values were replaced by one for representation on a log scale.

Figure 5 iNKT cell cytotoxicity associated with TB-IRIS

iNKT cells were characterised longitudinally by flow cytometric analysis for surface markers CD161 and CD107a, in TB-IRIS patients and non-IRIS patients . Between ARV0 and ARV2, CD161+ iNKT cells there was a reduction in CD161+ iNKT cell percentage in TB-IRIS compared to non-IRIS patients (A), whereas CD107a+ iNKT cell percentage increased in TB-IRIS patients between ARV0 and ARV2, compared to non-IRIS patients (B). CD107a+ iNKT cell frequency (cells per million CD3+CD19- live lymphocytes) was increased in TB-IRIS patients compared to non-IRIS controls at ARV2, the most common time of TB-IRIS presentation (C). Mann-Whitney U analysis for TB-IRIS vs non-IRIS: * $p<0.05$; ** $p<0.01$.

Table 1 Demographic and clinical features of the cross-sectional study participants

	HIV-TB-	*HIV-TB+*	*HIV+TB-*	*HIV+TB+*	*p value*
n	32	20	26	23	
Female, n (%)	14 (43.8)	7 (35.0)	15 (57.7)	9 (39.1)	>0.100[a]
Smoking status: current or ex,, n (%)	17 (53.1)	10 (50.0)	9 (34.6)	9 (39.1)	>0.100[a]
Age, median years (IQR)	29.0 (23.3-38.8)	38.0 (30.0-42.8)	32.5 (28.5-35.3)	31.0 (28.0-40.0)	0.059[b]
CD4 T cell count, median cells/ml (IQR)	N/A	N/A	349 (204-483)	187 (104-386)	0.041
CD4 T cell percentage, median (IQR)	N/A	N/A	17.8 (12.0-22.3)	13.7 (9.22-26.3)	0.901
HIV viral load, median copies/ml (IQR)	N/A	N/A	25735 (6807-92169)	296196 (13540-503097)	**0.031**
Symptomatic, n (%)	16 (50.0)	20 (100)	10 (38.5)	23 (100)	
Duration of symptoms, median days (IQR)	14.0 (4.00-150)	28.0 (14.0-30.0)	60.0 (11.3-82.5)	30.0 (21.0-30.5)	0.595[C]
Miliary TB, n (%)	0 (0)	0 (0)	0 (0)	5 (21.7)	0.051[d]
Extrapulmonary TB, n (%)	N/A	3 (15.0)	N/A	10 (43.5)	0.054[d]
Smear positive TB, n (%)	0 (0)	13 (65.0)	0 (0)	8 (34.8)	0.069[d]
Culture positive TB, n (%)	0 (0)	10 (50.0)	(0)	18 (78.3)	0.064[d]
Clinical diagnosis TB, n (%)	0 (0)	3 (15.0)	0 (0)	2 (8.70)	0.650
Cavitary disease on CXR, n (%)	0 (0)	14 (70.0)	0 (0)	9 (39.1)	0.067[d]

[a]for comparison between each group by Fisher's Exact test
[b]for comparison of all groups by Kruskal-Wallis test, Dunn's multiple comparisons test for a difference between HIV-TB- and HIV-TB+ (p=0.033)
[c]for comparison of all groups by Kruskal-Wallis test
[d]for comparison between HIV-TB+ and HIV+TB+ by Fisher's Exact test

Table 2 iNKT cell enumeration in cross-sectional study participants by diagnosis

Patient category				*Dunn's multiple comparisons test*				
HIV- TB-	*HIV- TB+*	*HIV+TB-*	*HIV+TB+*	*HIV- TB- vs. HIV- TB+*	*HIV- TB- vs. HIV+TB-*	*HIV- TB- vs. HIV+TB+*	*HIV+TB- vs. HIV+TB+*	*HIV- TB+ vs. HIV+TB+*
iNKT cell frequency, median per million CD3+CD19- live lymphocytes (IQR)								
1700 (1125, 2600)	735 (253, 1800)	375 (198, 1775)	280 (62.7, 1300)	0.149	**0.005**	**0.001**	>0.999	0.731
iNKT cell number, median cells per ml blood (IQR)								
282628 (151100, 487870)	88580 (29600, 203771)	44965 (19635, 219669)	24439 (3789, 119449)	**0.044**	**0.002**	**<0.001**	0.432	0.161
CD4+ iNKT cells, median percentage (IQR)								
44.5 (27.9, 61.1)	38.9 (16.3, 67.1)	13.67 (2.77, 39.2)	3.15 (0, 39.6)	>0.999	**0.005**	**<0.001**	>0.999	**0.007**
CD4+ iNKT cell frequency, median per million CD3+ CD19- live lymphocytes (IQR)								
712 (451, 1043)	202 (78.8, 601)	100 (11.5, 236)	18.9 (0, 148)	**0.016**	**<0.001**	**<0.001**	>0.999	**0.013**

561 **Table 3** Demographic and clinical features of participants in longitudinal study at enrolment
562

	TB-IRIS	*non-IRIS*	*p value*
n (%)	29 (63.0)	17 (37.0)	
Female, n (%)	14 (48.3)	10 (58.8)	0.552
Smoking status: current or ex-, n (%)	9 (31.0)	3 (17.5)	0.489
Age, median years (IQR)	35.0 (29.5-42.0)	35.0 (30.5-43.0)	0.924
CD4 T cell count, median cells/μl	89.0	82.0	0.987
(IQR)	(64.0-141.5)	(69.5-145.5)	
HIV-1 viral load, median copies/ml	621075	520295	0.343
(IQR)	(207018-1185455)	(126925-1029554)	
Extrapulmonary TB, n (%)	21 (72.4)	12 (70.6)	1.00
Miliary TB, n (%)	5 (17.2)	1 (5.88)	0.390
Smear positive TB, n (%)	14 (48.3)	5 (29.4)	0.235
Culture positive TB, n (%)	21 (72.4)	11 (64.7)	0.742
Clinical diagnosis TB, n (%)	2 (6.90)	4 (23.5)	0.174
ART initiation, days post TB treatment initiation	15	21	0.186
(IQR)	(14-28)	(14-41)	
IRIS symptom onset, median days post-ART	6	N/A	
initiation (IQR)	(4-10)		
IRIS presentation, median days post-ART initiation	14	N/A	
(IQR)	(9-15)		
INSHI[a] criteria for paradoxical TB-IRIS fulfilled, n	25 (86.2)	0 (0)	
(%)			

563

564 [a]International Network for the Study of HIV-associated IRIS
565
566
567

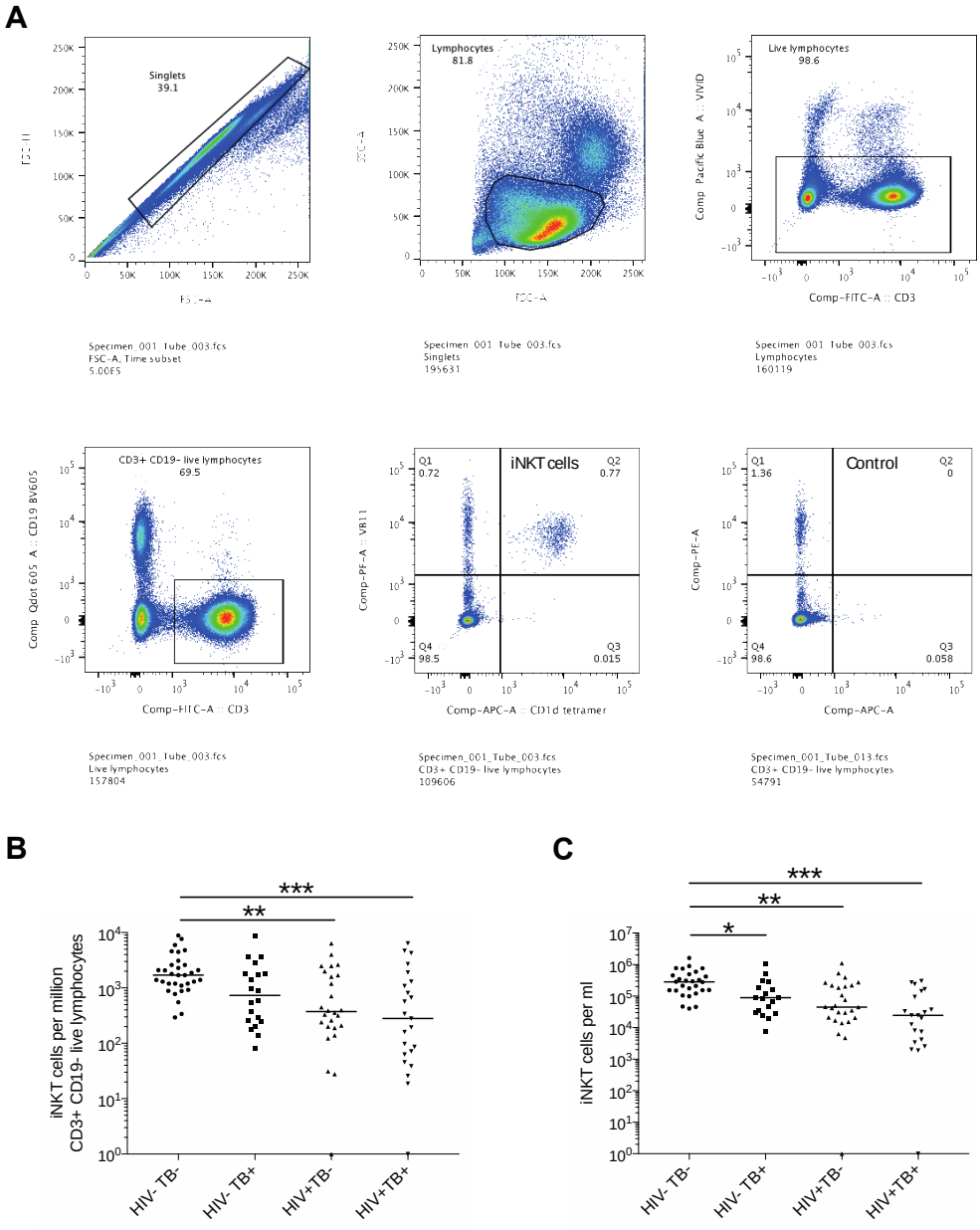
A
Singlets
39.1
Lymphocytes
81.8
Live lymphocytes
98.6
Comp-FITC-A :: CD3
CD3+ CD19- live lymphocytes
69.5
iNKT cells
Q1
0.72
Q2
0.77
Q4
98.5
Q3
0.015
Comp-APC-A :: CD1d tetramer
Control
Q1
1.36
Q2
0
Q4
98.6
Q3
0.058
B
iNKT cells per million
CD3+ CD19- live lymphocytes
HIV- TB-
HIV- TB+
HIV+TB-
HIV+TB+
C
iNKT cells per ml
HIV- TB-
HIV- TB+
HIV+TB-
HIV+TB+

Figure 1

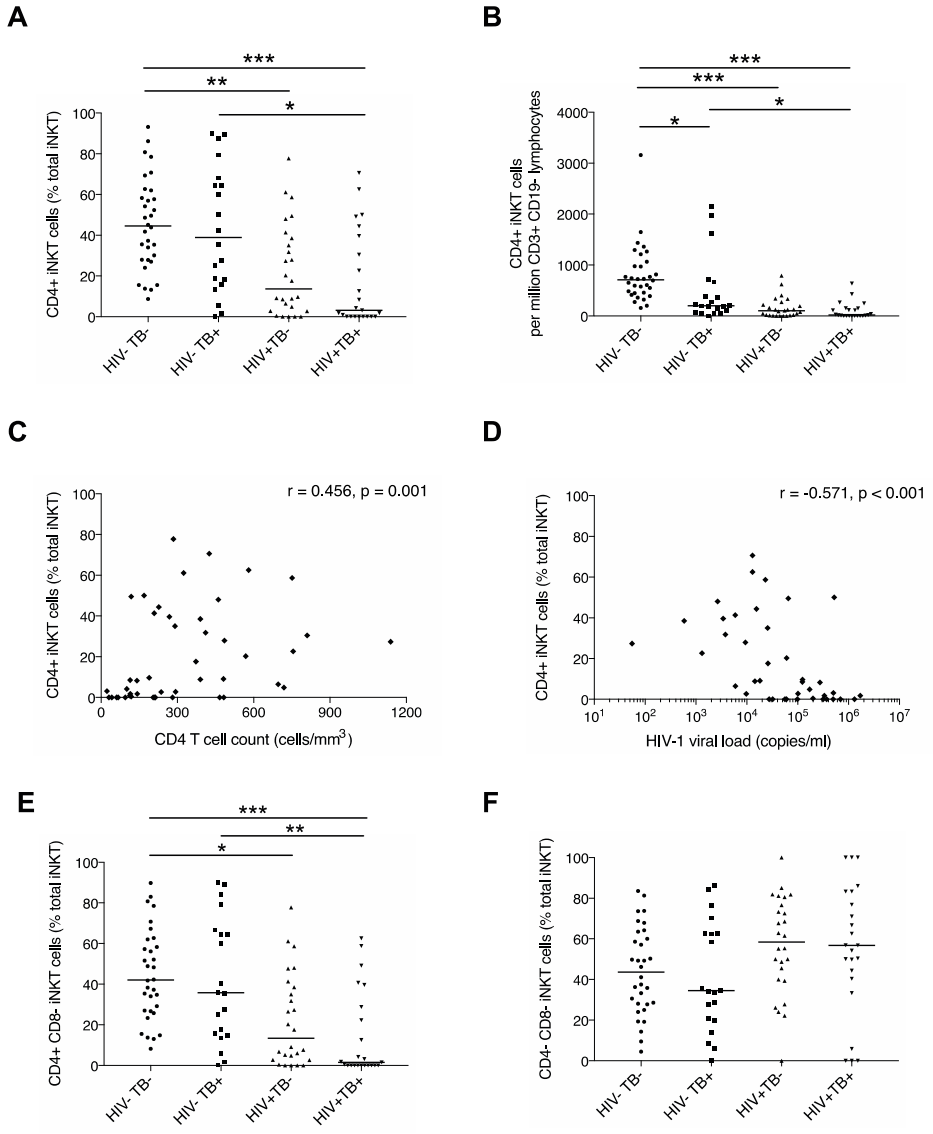
A
B
C
D
E
F
CD4+ iNKT cells (% total iNKT)
CD4+ iNKT cells per million CD3+ CD19- lymphocytes
CD4+ CD8- iNKT cells (% total iNKT)
CD4- CD8- iNKT cells (% total iNKT)
HIV- TB-
HIV- TB+
HIV+TB-
HIV+TB+
r = 0.456, p = 0.001
CD4 T cell count (cells/mm3)
r = -0.571, p < 0.001
HIV-1 viral load (copies/ml)

Figure 2

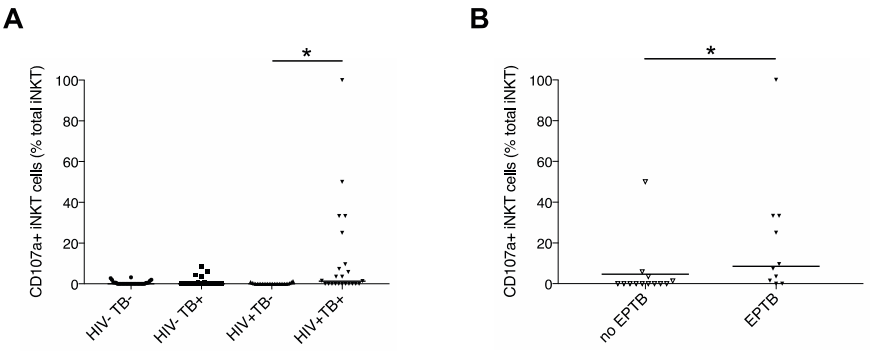

579
580
581
582 **Figure 3**
583

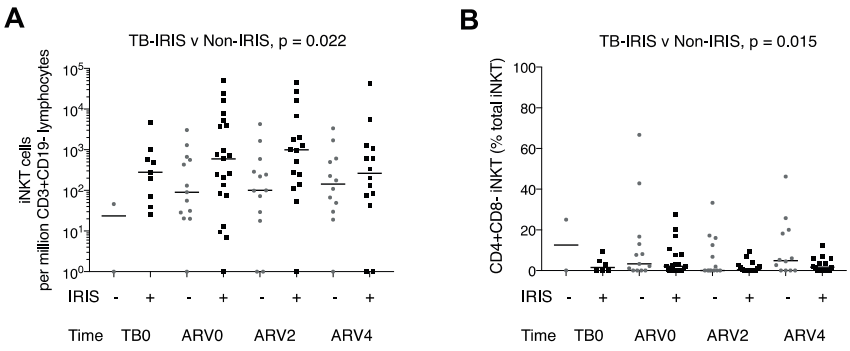

584
585
586
587
588 **Figure 4**
589

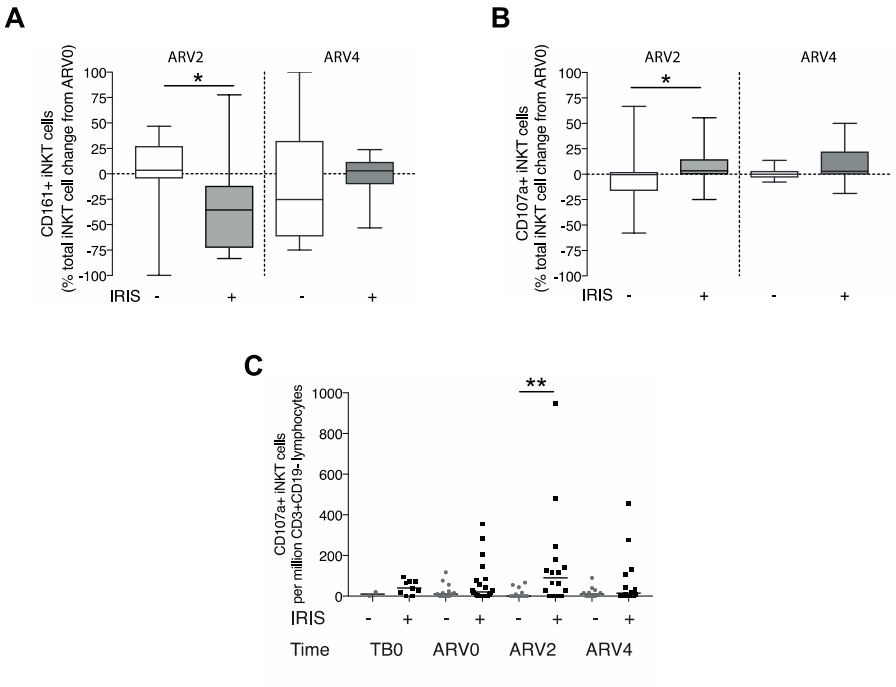
A
ARV2
ARV4
*
CD161+ iNKT cells
(% total iNKT cell change from ARV0)
100
75
50
25
0
-25
-50
-75
-100
IRIS - + - +
B
ARV2
ARV4
*
CD107a+ iNKT cells
(% total iNKT cell change from ARV0)
IRIS - + - +
C
**
CD107a+ iNKT cells
per million CD3+CD19- lymphocytes
1000
800
600
400
200
0
IRIS - + - + - + - +
Time TB0 ARV0 ARV2 ARV4

Figure 5

Online Data Supplement

Invariant Natural Killer T cell dynamics in HIV-associated tuberculosis

Invariant Natural Killer T cells in TB-IRIS

Walker NF, Opondo C, Meintjes G, Jhilmeet N, Friedland JS,

Elkington PT, Wilkinson RJ, Wilkinson KA.

Materials and Methods

Study Participants and clinical assessment

The study was approved by the University of Cape Town Human Research Ethics Committee (REF 516/2011) and conducted in accordance with the Declaration of Helsinki. Cross-sectional study participants were recruited in an outpatient clinic in Khayelitsha, South Africa and were either healthy volunteers, patients with symptoms requiring assessment, or recently diagnosed TB patients. HIV-infected patients were ART naive at enrolment. Cross-sectional study participants who were on anti-tuberculosis therapy were required to have had less than 3 doses prior to study samples being collected. Once enrolled, cross-sectional study participants were provided appropriate follow up by the research team for study clinical results and were then followed up routinely by clinic staff, unless also eligible for the longitudinal study.

Cross-sectional study participants were retrospectively designated into four categories:

1) HIV-uninfected patients without active TB (HIV-TB-)

2) HIV-uninfected patients with a new diagnosis of active TB (HIV-TB+)

3) ART naïve, HIV-infected patients without active TB (HIV+TB-)

4) ART naïve, HIV-infected patients with a new diagnosis of active TB (HIV+TB+).

Active TB was diagnosed on the basis of smear or culture positivity, or in cases of smear-negative TB according to international guidelines [1, 2]. This required suggestive symptoms

and at least one of:

a) Sputum smear positive for acid fast bacilli on microscopy (Smear positive)
b) Sputum Gene Xpert-RIF (Cepheid, Sunnyvale, CA) positive for *Mycobacterium tuberculosis* (Mtb)
c) Sputum culture positive for Mtb (Culture-confirmed)
d) Clinical features highly suggestive of TB such as diagnostic features on chest radiograph or other imaging modality and a decision to start TB treatment by the treating clinician (Clinical diagnosis)

Cross-sectional study participants who had symptoms but did not meet the criteria for TB diagnosis were designated controls if there was a low clinical suspicion for active TB and they had at least one induced sputum smear negative for acid fast bacilli and one induced sputum culture that was negative for Mtb. These patients were not started on anti-tuberculosis therapy. All HIV-infected patients who were designated non-TB controls also had at least one induced sputum smear negative for acid fast bacilli and one induced sputum culture that was negative for Mtb. HIV-infected active TB patients in the cross-sectional study who met eligibility criteria for the longitudinal study were co-enrolled, or if eligibility became apparent after enrolment, were invited to subsequently participate in the longitudinal study.

Longitudinal study participants were ART naïve HIV-infected patients with a low CD4 count (<200 cells/mm^3) and a recent diagnosis of active TB. Following anti-tuberculosis therapy initiation and enrolment into the longitudinal study (study visit TB0) patients received counselling for ART initiation. Anti-tuberculosis therapy and ART followed national guidelines [3, 4]. First-line ART at the time of the study was principally tenofovir, lamivudine, and

efavirenz. ART was initiated typically two weeks after anti-tuberculosis therapy (study visit ARV0) and patients attended further scheduled study visits at two weeks post-ART initiation (ARV2, Day 14 +/- 72 hours) and four weeks post-ART initiation (ARV4, Day 28 +/-72 hours) for clinical assessment and sampling. Patients who had taken more than four doses of TB treatment at enrolment contributed samples from ARV0.

Patients were requested to attend for assessment if any new symptoms or clinical deterioration occurred (study interim assessment) and were followed up to twelve weeks post-ART initiation. Clinical research staff telephoned participants regularly to reinforce this, to remind patients about scheduled visits and to investigate non-attendance. If a case of TB-IRIS was suspected, study samples were collected as at a scheduled visit, in addition to clinically indicated diagnostic tests. Where possible, when patients were hospitalized at the time of a study visit, they were visited by the study team for data and sample collection. Retrospective designation into one of three longitudinal study categories (paradoxical TB-IRIS (INSHI IRIS), probable paradoxical TB-IRIS not meeting INSHI criteria (IRIS non-INSHI), and no paradoxical TB-IRIS (non-IRIS)) followed the results of all relevant investigations and clinical follow up, and was made on case review by a consensus panel (comprising the study clinician NFW, and two clinical specialists: GM, RJW). Designation as TB-IRIS included both INSHI-IRIS and non-INSHI IRIS.

In both cross-sectional and longitudinal studies, demographic information was recorded at enrolment, including gender and smoking status. At each study visit, symptoms and clinical examination, full blood count, albumin, C-reactive protein (CRP) and chest radiograph were

performed, plus additional investigations if clinically indicated. Induced sputum and venous blood were collected (see below) at each visit for microbiological and laboratory analysis.

Venous blood for PBMC isolation was collected in sodium heparin vacutainers, transported at room temperature to UCT, and processed within four hours of collection. PBMC were isolated by layering over Ficoll and cryopreserved in heat-inactivated fetal calf serum (FCS) with 10% dimethyl sulfoxide (DMSO) until used in batches.

Additional venous blood sample analysis was performed by the National Health Laboratory Service (NHLS), including full blood count and differential measured using a Siemens Advia 2120I (Siemens, Surrey, UK), albumin and C-reactive protein (CRP) quantification on a Roche Modular (F. Hoffman-La Roche Ltd) and for HIV-infected patients, CD4 count measured on a Beckman Coulter FC500MP (Beckmann Coulter, Inc, Buckinghamshire, UK) and HIV-1 viral load measured on an Abbott M2000 (Abbott Analytical Limited, London, UK). Induced sputum was collected for microscopy and mycobacterial culture.

CD1d Tetramer staining

Cryopreserved PBMC were rapidly thawed in warmed RPMI/10% FCS and washed. All wash steps consisted of centrifugation at 1500 rpm for 5 minutes, discarding of supernatant and disruption of the cell pellet by vortex. PBMC were counted using a Bio-rad TC20^{TM} automated cell counter and viability was ascertained by trypan blue exclusion. For iNKT cell enumeration, one million cells per tube were transferred into two labelled fluorescence activated cell

sorting (FACS) tubes per patient: one for α-galcer-loaded CD1d tetramer and one for CD1d (control) tetramer staining for each sample. Cells were washed in PBS and resuspended for viability staining with Violet LIVE/DEAD© Fixable stain kit (VIVID, Invitrogen, Paisley, UK) (1:1000 dilution, 200µl per tube) and incubated for 30 minutes at 4°C in the dark. They were then washed in PBS and resuspended in 30µl cold PBS prior to tetramer staining with α-galcer-loaded CD1d tetramer (tet+) or control CD1d tetramer (tet-cont) (Proimmune, Oxford, UK), added at 0.5ul per tube and then incubated for 30 minutes on ice. Tet+ and tet-cont-stained cells were protected from light at all times.

Characterisation by cell surface marker expression

Following tetramer staining, cells for surface marker characterisation were stained with an antibody mastermix containing CD3, CD19, CD4, CD8, CD107a, CD95, CD161, CD40L, PD1, and Vβ11 for 30 minutes at 4°C (see Supplementary Table S1). They were then washed and re-suspended in PBS, 1% Hi-FCS, 2% paraformaldehyde for 1 hour. After a further wash, cells were re-suspended in 300µl wash buffer and acquired on an LSR Fortessa (BD Biosciences) within 24 hours of staining. Single fluorochrome-stained positive and negative control compensation beads were acquired for each experiment to enable fluorescence compensation. Data were analysed using Flowjo software (Tree Star, Ashland, OR).

iNKT cell frequency was calculated as a percentage of CD3+ CD19- live lymphocytes, with subtraction of the equivalent tet-cont proportion, and reported per million CD3+CD19- live lymphocytes. Negative values were reassigned zero for analysis. Zero values were assigned 1

if graphically represented on a log scale. Absolute iNKT cell numbers were calculated by multiplying the iNKT cell count, as a percentage of live lymphocytes, with the total lymphocyte count per milliliter of peripheral blood, as previously reported [5]. Phenotypic characteristics of iNKT cells are reported as the iNKT cell percentage expressing cell surface markers (CD4, CD8, CD107a, CD95, CD161, CD40L, PD1). This proportion was multiplied by the total iNKT cell frequency to give the iNKT cell subset frequency.

Statistical analysis

Flow cytometry data was analysed using Flowjo software (Treestar, USA). Gating was determined by comparison to samples stained by the control tetramer or fluorescence-minus-one controls. Statistical analysis was performed using Prism 6 (GraphPad, UK) and STATA version 14. Unadjusted non-parametric analyses were by two-tailed Fisher's Exact or Mann–Whitney U, or for comparisons of more than two groups, by Kruskal-Wallis with Dunn's multiple comparisons test. Comparison of total CD4 count changes over time in the longitudinal study was by two-way repeated measures ANOVA. In the cross-sectional study, we used a multivariable linear regression model to investigate differences in iNKT cell frequency and percentage CD4/CD8 expression by disease category. In the longitudinal study, a multivariable negative binomial model was fitted to examine the association of iNKT frequency with TB-IRIS status and a multivariate linear regression model was used to estimate the difference in CD4/CD8 cell subset percentages between TB IRIS and non-IRIS patients. Data from scheduled visits, ARV0, ARV2 and ARV4 was included in this analysis and ARV0 was used as the baseline timepoint.

Supplementary References

1. Siddiqi K, Lambert ML, Walley J. Clinical diagnosis of smear-negative pulmonary tuberculosis in low-income countries: the current evidence. Lancet Infect Dis **2003**; 3(5): 288-96.
2. WHO. Improving the diagnosis and treatment of smear-negative pulmonary and extra-pulmonary tuberculosis among adults and adolescents: recommendations for HIV-prevalent and resource-constrained settings. World Health Organisation, Geneva, **2006**.
3. The South African Antiretroviral Treatment Guidelines 2013. Department of Health, Republic of South Africa, **2013**.
4. National Tuberculosis Management Guidelines 2014: Department of Health, Republic of South Africa 2014.
5. Kee SJ, Kwon YS, Park YW, et al. Dysfunction of Natural Killer T Cells in Patients with Active *Mycobacterium tuberculosis* Infection. Infect Immun **2012**; 80(6): 2100-8.

Supplementary Figure Legends

Supplementary Figure S1 iNKT cell enumeration in cross-sectional study participants

iNKT cells were enumerated using α-galcer-loaded CD1d tetramers and control CD1d tetramers (no α-galcer). Gating on CD3+ CD19- live lymphocytes generated the plots shown. For each participant, peripheral blood mononuclear cells were stained using α-galcer-loaded CD1d tetramers (column A) in parallel with a control tetramer (column B). iNKT cells (shown in Q2, column A) were defined as CD3+ CD19- CD1d α-galcer tet+ Vβ11+ T cells and enumerated by subtraction of non-specific tetramer staining in the equivalent control gate (Q2 column B). Representative plots are shown for each of the four patient categories in the cross-sectional study: HIV-uninfected patients without active TB (HIV-TB-); HIV-uninfected patients with active TB (HIV-TB+); HIV-1-infected patients without active TB (HIV+TB-); HIV-1-infected patients with active TB (HIV+TB+).

Supplementary Figure S2 CD4 and CD8 iNKT cell subset frequency in cross-sectional study patients

CD4+CD8- iNKT cell subset frequency (cells per million CD3+CD19- live lymphocytes) was reduced in HIV infection and in active TB in HIV-uninfected patients (A). There was reduced CD4-CD8- iNKT cell frequency in HIV-infected patients with active TB compared to HIV-uninfected patients without active TB (B). There was no difference in iNKT cell frequency of CD-CD8+ (C) or CD4+ CD8+ (D) iNKT cell frequency between HIV-infected and uninfected patients, with and without active TB. Analysis was by Kruskal Wallis with Dunn's multiple comparison's test to calculate multiplicity adjusted p values: *$p<0.05$; **$p<0.01$; ***$p<0.001$.

Supplementary Figure S3 iNKT cell numbers in longitudinal study patients

iNKT cells were enumerated by flow cytometry using α-galcer loaded CD1d tetramers, in a cohort of 46 HIV-1-infected patients with active TB. Following TB diagnosis (TB0), TB treatment was initiated. Anti-retroviral therapy was initiated at ARV0, a median of 17.5 days post TB treatment initiation. Patients who had taken more than four doses of TB treatment at enrolment contributed data from ARV0, resulting in fewer data points at TB0. Additional study visits occurred at two (ARV2) and four (ARV4) weeks post-ART initiation. TB-IRIS presentation was typically at ARV2. iNKT cell numbers were calculated by multiplying the iNKT cell count, as a percentage of live lymphocytes quantified by flow cytometry, with the total lymphocyte count per millilitre of peripheral blood as recorded on the full blood count. There was a trend towards increased iNKT cell numbers in TB-IRIS patients compared to non-IRIS controls in the age and sex-adjusted multivariate model (p=0.062). Zero values were replaced by one for representation on a log scale.

Supplementary Figure S4 CD4 negative iNKT cell subsets predominate in TB-IRIS and non-IRIS patients

CD4-CD8- and CD4-CD8+ iNKT cell subset percentage (A, B) and iNKT cell frequency per million CD3+ CD19- live lymphocytes (C, D) are shown. CD4-CD8- iNKT cells were the most abdundant as a percentage of total iNKT cells (A), followed by CD4-CD8+ iNKT cells (B) in both TB-IRIS and non-IRIS patients. However, in TB-IRIS patients CD4-CD8- (C) and CD4-CD8+ (D) iNKT cell frequency was increased compared to non-IRIS patients at ARV2, the usual time of IRIS presentation. CD4+CD8+ iNKT cells were infrequent (data not shown). Zero values were

replaced by 0.1 for representation on a log scale. Analysis was by Mann Whitney-U comparing TB-IRIS with non-IRIS at each timepoint: *p<0.05.

Supplementary Figure S5 iNKT cell phenotype in HIV-associated TB

iNKT cells where characterized by proportional surface expression of CD161, CD107a, CD95, PD1 and CD40L, indicating maturation, degranulation, cytotoxicity, anergy and activation, respectively. CD161+ (A) and CD107a+ (B) iNKT cell proportions were dynamic. CD95+ iNKT cell proportions were very high in both TB-IRIS and non-IRIS patients (C). PD1+ iNKT cell proportions were relatively high (E) whereas CD40L+ iNKT cell proportions were relatively low, possibly indicating an exhausted state (F). Individual patient data are shown and consecutive visits are joined by a line. Routine study visits were at ARV0 (anti-retroviral therapy initiation), ARV2 and ARV4 (two and four weeks post-ART initiation). Unscheduled study visits indicating new symptoms were at ARV1 and ARV3 (one and three weeks post-ART initiation).

Supplementary Tables

Supplementary Table S1 Flow cytometry panel for iNKT cell enumeration and phenotype, comprising LIVE/DEAD© Fixable stain (VIVID), either α-galcer-loaded CD1d tetramer or control CD1d tetramer and antibodies for cell surface markers (surface antibody mastermix 1).

Surface Marker	Function	Fluorochrome	Volume/million PBMC stained (μl)
	Viability	VIVID	200 (1:1000)
CD3	Identify T cells	FITC	1
CD19	Gate out B cells	BV510	3
CD1d tetramer	iNKT cell identification	APC	0.5
VB11		PE	5
CD4	Assess functional maturity & Th1 (CD4+/-)/Th2 (CD4+) polarisation	PerCP-Cy5.5	5
CD8	Cytotoxicity (CD8+)	APC-H7	1
CD161 (NK1.1)	Activation / maturation	BV510	5
	NK marker		
CD107a	Degranulation	Alexa Fluor 700	5
CD95	Fas- Fas ligand mediated cytotoxicity	BV711	5
PD-1	Induction and maintenance of iNKT cell anergy (in TB)	PE-Cy7	5
CD40L (CD154)	Activation	PE-CF594	5
	Interaction with innate immune cells / B cells		

Supplementary Table S2 Multivariable linear regression model of CD4/CD8 percentage expression on iNKT cells in the cross-sectional cohort by clinical category in comparison to HIV-uninfected controls without active TB (HIV-TB-), adjusted for age and sex.

		Coefficient	95% CI	p value
CD4-CD8+				
	HIV-TB+	4.92	-3.58, 13.4	0.257
	HIV+TB-	6.97	0.42, 13.5	**0.037**
	HIV+TB+	12.4	2.28, 22.5	**0.016**
CD4+CD8+				
	HIV-TB+	-0.38	-2.49, 1.73	0.725
	HIV+TB-	-0.39	-1.18, 0.40	0.334
	HIV+TB+	2.22	-1.87, 6.31	0.288
CD4+CD8-				
	HIV-TB+	-4.00	-17.9, 9.91	0.573
	HIV+TB-	-23.8	-33.7, -13.8	**<0.001**
	HIV+TB+	-30.5	-41.3, -19.6	**<0.001**
CD4-CD8-				
	HIV-TB+	0.45	-13.2, 14.1	0.949
	HIV+TB-	13.6	3.31, 23.8	**0.010**
	HIV+TB+	11.8	-4.45, 28.0	0.155

Supplementary Table S3 Multivariable negative binomial model assessing relationship between iNKT cell frequency and TB-IRIS status.

Unadjusted	Coefficient	95% CI	p value
	3.99	1.18, 13.5	**0.026**
Adjusted[a]	Coefficient	95% CI	p value
	4.13	1.23, 13.9	**0.022**

[a]adjusted for age and sex

Supplementary Table S4 Multivariate linear regression model to estimate the difference in CD4/CD8 cell subset percentage between TB IRIS and non-IRIS patients, adjusted for time.

	Difference in cell subset percentage (TB-IRIS vs non-IRIS)	95% CI	p value
CD4-CD8+	-3.02	-14.4, 8.36	0.603
CD4+CD8+	1.03	-10.5, 12.6	0.861
CD4+CD8-	-6.64	-12.0, -1.28	**0.015**
CD4-CD8-	8.63	-5.49, 22.2	0.231

Supplementary Figures

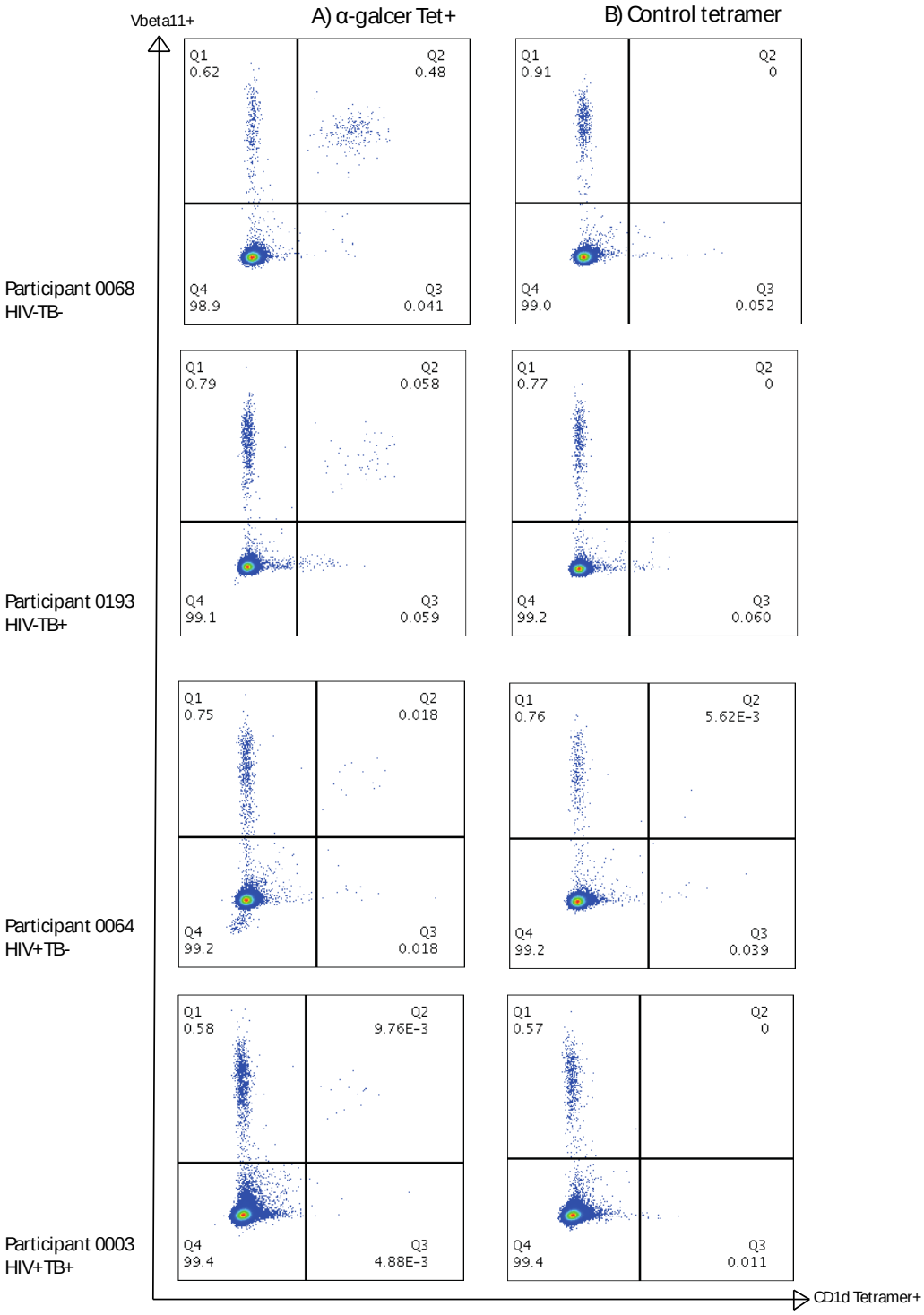

Supplementary Figure S1

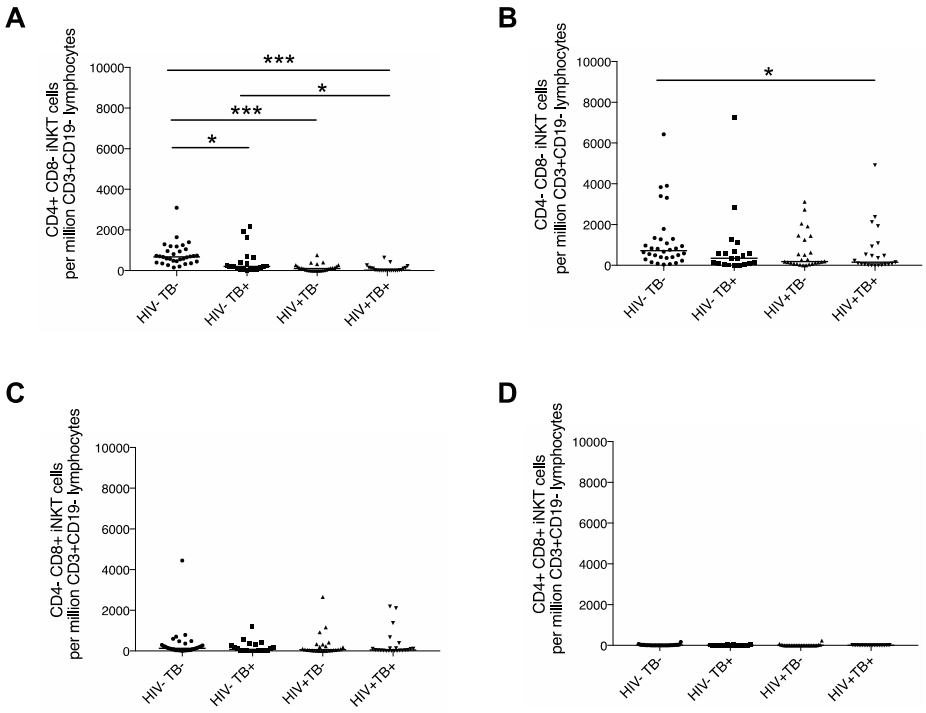

Supplementary Figure S2

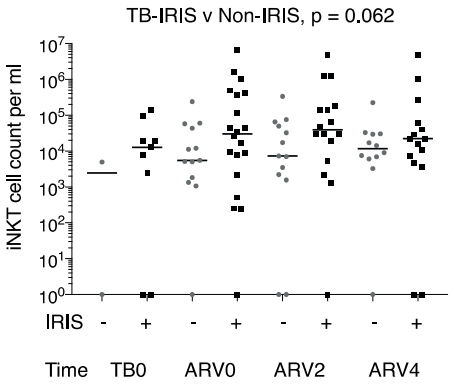

Supplementary Figure S3

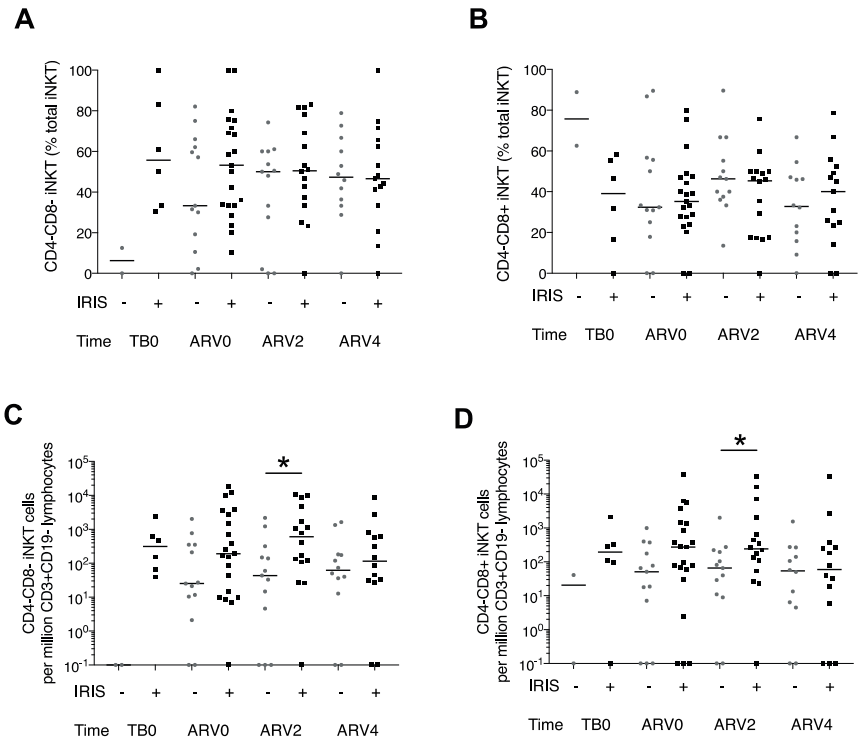

Supplementary Figure S4

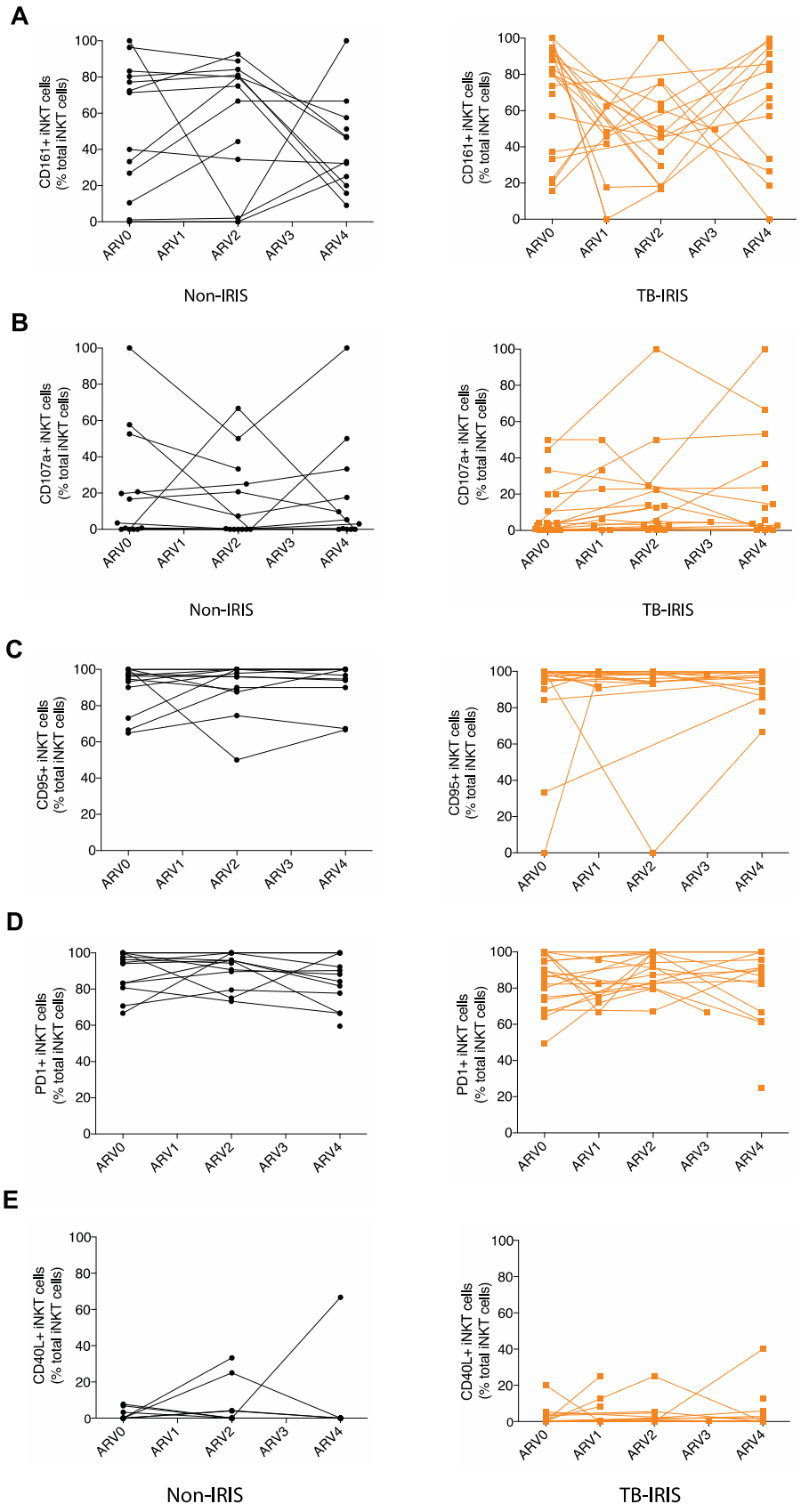

Supplementary Figure S5